MAGNETOHYDRODYNAMICS Vol. 53 (2017), No. 3, pp. 449–459

DYNAMICS OF A SUPERPARAMAGNETIC MICROPARTICLE CHAIN IN AN OSCILLATING MAGNETIC FIELD: EFFECTS OF FIELD FREQUENCY

Ching-Yao Chen[1], *He-Ching Lin*[2], *Che-Jui Teng*[1], *Yan-Hom Li*[3]

[1] *Department of Mechanical Engineering, National Chiao Tung University, Hsinchu City, Taiwan R.O.C.*

[2] *Department of Mechanical Engineering, Air Force Institute of Technology, Kaohsiung, Taiwan R.O.C.*

[3] *Department of Mechanical and Aerospace Engineering, National Defense University, Taoyuan, Taiwan R.O.C.*

e-Mail: chingyao@mail.nctu.edu.tw

Dynamics of an oscillating chain consisting of several magnetic microparticles and driven by oscillating magnetic fields with different frequencies are discussed. Because of a shorter driving time by the external field with a higher field frequency, the oscillating amplitude of the chain reduces. On the other hand, the higher field frequency leads to a faster local angular velocity. These two effects result in inconsistent behavior of the structural stability of the chain, so that the chain ruptures in a field of intermediate frequency. A dimensionless parameter of the reduced frequency is proposed to generally describe the monotonic decrease of the normalized amplitude. The phenomenon of trajectory shift triggered by the higher frequency field is also demonstrated.

Introduction. In the past decades, magnetorheological (MR) suspensions, in which nano-sized or micro-sized superparamagnetic solid particles are suspended in a nonmagnetic solvent, are actively applied in the so-called magnetofluidics [1]. For more detailed progresses regarding the magnetic particle based applications, the readers are referred to the comprehensive reviews [2, 3]. Among the applications, micro-devices formed by particles and manipulated by external fields have attracted significant interests of researches, e.g., sensors [4, 5], swimmers [6–10], mixers [11–13], and components in micro-electromechanical systems (MEMS) [14–18]. In the meantime, to ensure the applicability of these micro-devices, chaining processes and dynamics of micro-chains in motion must be well understood. Intensive studies of chains driven by dynamical fields have been carried out, e.g., in a rotational field [19–33] and in an oscillating field [34–37].

It has been successfully demonstrated that micro-swimmers can be composed and manipulated in an oscillating field [6–10]. In the pioneer work on the formation of a magnetic micro-swimmer [6], DNA is used to strongly bond the magnetic particles. On the other hand, an easier and reversible procedure of micro-swimmer formation is also presented when a swimmer is designed simply by chaining the magnetic particles of different sizes [8–10]. Nevertheless, structural instability, i.e., chain rupture, might occur in this configuration because of weaker bonding magnetic forces. To better understand the structural instability, a criterion of rupture can be effectively predicted by the value of $N\sqrt{\mathrm{Mn}}$, where Mn and N, respectively, stand for the dimensionless Mason number and the number of particles constituing the chain. Under this particular configuration, to maintain the stable chain formationa, critical value of $N\sqrt{\mathrm{Mn}} < 1.7 \sim 2$ is suggested [34, 35]. Detailed patterns and timings of the structural instability are also thoroughly categorized [37]. Meanwhile, interesting phenomena observed at high field strengths, referred to as the trajectory shift, are identified if the instantaneous phase difference between

the chain and the external field is more than 90° [35]. By this trajectory shift, swimmers can be steered to move perpendicularly by a rapid increase of the field strength [9, 35].

An important issue concerning the application of micro-swimmers is the improvement of the swimmer efficiency. It is commonly understood that the efficiency is strongly related to the structural stability and amplitude of the oscillating chain. The structural instability of a ruptured chain is certainly undesired during the swimming motion. On the other hand, to maximize the propulsive force, a higher oscillating amplitude is generally preferred. Nevertheless, these two factors often appear to be contradictory. The higher amplitude tends to increase the local angular velocity of the oscillating chain, hence, increases the possibility of a ruptured chain. As a result, the amplitude appears to be a crucial factor of the swimming efficiency. Significant results regarding the oscillation amplitude and the structural rupture were presented in the early literature [34, 35, 37]; the quantitative data were obtained under fixed conditions of lower frequency, e.g., $f = 1\,\mathrm{Hz}$. In the present study, the influence of the field frequency on the oscillating amplitude is experimented. A generalized dimensional analysis of a normalized amplitude is emphasized. In addition, patterns of the oscillations of micro-chains at various frequencies will be also addressed.

1. Experimental setup. Fig. 1 shows the principle sketch of the experimental setup and the relevant notations. Micro-sized superparamagnetic particles, whose mean diameters are $d = 4.5\,\mu\mathrm{m}$ with an initial susceptibility of $\chi = 1.6$ are dispersed in a mixture of distilled water and sodium dodecyl sulfate (SDS) surfactants. The viscosity of such mixture is $\eta = 1.75\,\mathrm{cp}$. A static directional magnetic field, denoted as $\mathbf{H}_\mathrm{d}$, is first applied horizontally to form a micro-chain. The chain formed by N particles is referred to as a PN chain, e.g., a representative P8 chain ($N = 8$) shown in Fig. 1. Upon successful formation of a particle chain, an additional dynamic field ($\mathbf{H}_\mathrm{v}$) is applied vertically to drive the chain oscillation along the horizontal axis. The strength of the dynamic field is sinusoidal

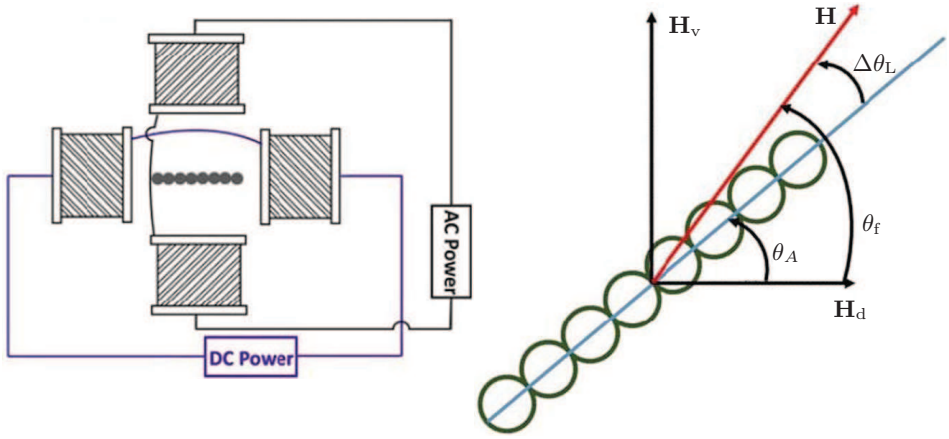

Fig. 1. Principle sketch of the experimental setup (left) and relevant notations (right). A static directional magnetic field ($\mathbf{H}_\mathrm{d}$) generated by a DC power source is applied horizontally to form a chain. An additional sinusoidal field ($\mathbf{H}_\mathrm{v}$) powered by an AC source is applied vertically. These two field components result in an oscillating external field $\mathbf{H}$. Instantaneous phase angles of the field and chain are denoted as θ_f and θ_A, respectively. The lagging angle of the chain to the field is represented as $\Delta\theta_\mathrm{L}$.

given by $H_v = H_p \sin(2\pi ft)$ with a maximum strength H_p and a frequency f. This results in an overall external field $\mathbf{H} = H_d\mathbf{i} + H_v\mathbf{j}$, in which $\mathbf{i}$ and $\mathbf{j}$ are the unit vectors in the directional (or horizontal) and vertical axes, respectively. Hence, the trajectory phase angle of the oscillating field denoted as θ_f can be determined as $\theta_f(t) = \tan^{-1}[(H_p/H_d)\sin(2\pi ft)]$ with an oscillating amplitude of $\theta_{fmax} = \tan^{-1}(H_p/H_d)$. The motion of the micro-chain is recorded by an optical microscope connected to a digital camera (Silicon Video 643C). Representative snapshots which are modified from the original recorded movies by improving their contrasts and resolutions are analyzed in the following sections to ascertain particular behaviors of the micro-chain exposed to various experimental conditions.

2. Results and discussion.

2.1. Structural instability and oscillating amplitude. Sequential images of a representative series of a P15 chain are shown in Fig. 2. The field strengths are fixed at $H_d = 24.15$ Oe and $H_p = 18.73$ Oe with various frequencies (*a*) $f = 1$ Hz, (*b*) 3 Hz and (*c*) 7 Hz. As a typical condition, $f = 1$ Hz is shown in the left column. The chain firstly moves clockwise, e.g., the image taken at $t = 0.25$ s, and then it moves counter-clockwise at $t = 0.5$ s and 0.75 s. Clockwise movement is resumed at $t = 1$ s to complete the entire period of oscillation. By visual inspection of these three cases, two apparent features of the oscillating chain influenced by varying the frequency can be observed, i.e. (1) the oscillating amplitude, and (2) the

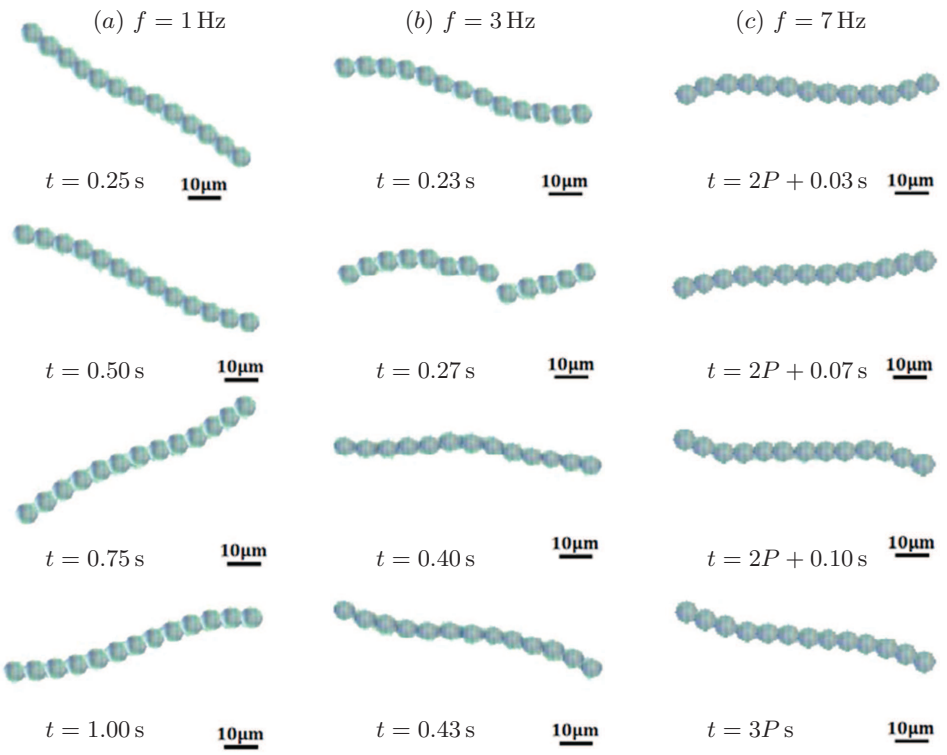

Fig. 2. Sequential images of a chain consisting of 13 particles (P13 chain) subjected to the field strengths $H_d = 24.15$ Oe and $H_p = 18.73$ Oe with increasing frequency (*a*) $f = 1$ Hz, (*b*) 3 Hz and (*c*) 7 Hz. The images for the case $f = 7$ Hz are snapshots between the second and the third oscillating period, in which P represents the period of oscillation, i.e. $P = 1/7$ s. The oscillating amplitude decreases with increasing frequency. Nevertheless, structural instability is observed at the intermediate frequency $f = 3$ Hz.

formation of chaining. Even if the chain oscillates with the same frequency as its correspondent external field, the amplitude is seen to decrease with increasing field frequency. On the other hand, the influence of the field frequency on the structural instability of the chain is not monotonic. While the chain preserves its stable chaining formation at the lower frequency $f = 1\,\mathrm{Hz}$, it appears continuously ruptured and re-chained if the field frequency is raised to $f = 3\,\mathrm{Hz}$. Nevertheless, the chain remains stable without rupture once the frequency is further raised to $f = 7\,\mathrm{Hz}$.

A smaller oscillating amplitude with a higher frequency can be realized by inspecting the phase trajectories of the external field (θ_f) and chain (θ_A) shown in Fig. 3. The field starts o oscillate clockwise so that the phase angle is negative within the first half of the period, i.e. $\theta_\mathrm{f} < 0°$ at $0\,\mathrm{s} < t < 0.5\,\mathrm{s}$ for the case with $f = 1\,\mathrm{Hz}$ illustrated in Fig. 3. Because of the stationary inertia effect and induced hydrodynamic drag, the trajectory phase angle of the oscillating chain would lag the external field by $\Delta\theta_\mathrm{L}$. It was noticed that this phase lag is the source driving the chain into oscillation, and the magnetic torque (M^m) is expressed as [26]

$$M^\mathrm{m} = \frac{\mu_0}{4\pi}\frac{3m^2N^2}{2(2a)^3}\sin(2\Delta\theta_\mathrm{L}). \tag{1}$$

Here μ_0 and a stand, respectively, for the vacuum permeability and for the radius of a magnetic particle. The dipolar moment m of a single particle is given by $m = \frac{4}{3}\pi a^3\chi H$. By the above expression, the magnetic torque changes the acting direction at $\Delta\theta_\mathrm{L} = 0°$. Hence, the chain would move reversely shortly after cross-over of the two trajectories, as illustrated in Fig. 3. As a result, the amplitude of the oscillating chain, denoted as θ_Amax, is expected to be smaller for a fixed field

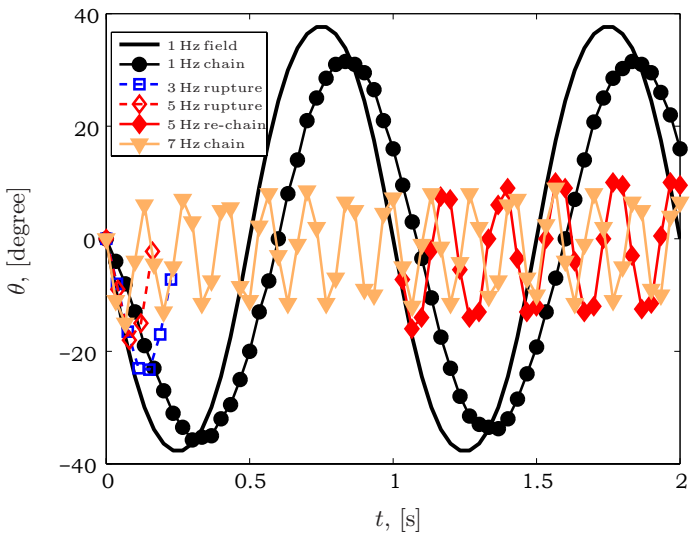

Fig. 3. Phase trajectories of the P13 chain shown in Fig. 2 for the frequencies $f = 1\,\mathrm{Hz}$, $3\,\mathrm{Hz}$, $5\,\mathrm{Hz}$ and $7\,\mathrm{Hz}$. Also shown is the field trajectory at $f = 1\,\mathrm{Hz}$. The maximum phase angle (or amplitude) of the oscillating chain occurs shortly after the cross-over of the trajectories of the field and chain, as shown in the case $f = 1\,\mathrm{Hz}$. The oscillating amplitude of the chain decreases as the field frequency increases. Chain ruptures within the first period of oscillation for the cases $f = 3\,\mathrm{Hz}$ and $5\,\mathrm{Hz}$. Nevertheless, for the case $f = 5\,\mathrm{Hz}$ the stable chaining formation is resumed after a few periods, e.g., $t > 1\,\mathrm{s}$.

strength if the cross-over of the trajectories occurs sooner, which is exactly the situation in a higher frequency field.

On the other hand, the influence of the field frequency on the chaining structural stability is inconsistent. As mentioned above, the chaining stability can be described well by the magnitude $N\sqrt{\mathrm{Mn}}$, where the dimensionless Mason number Mn is defined as [34, 35, 37]

$$\mathrm{Mn} = \frac{32\eta\omega}{\mu_0\chi^2 H^2}. \tag{2}$$

To maintain a stable chain without structural instability, a smaller value of $N\sqrt{\mathrm{Mn}}$ is preferred. To calculate the Mason number, the angular velocity ω is approximated by the amplitude of oscillation, e.g., $\omega \approx 4f\theta_{\mathrm{Amax}}$ [34, 35, 37]. With this approximation, it is clear that the frequency results in a contradictory effect on the structural stability of the chain, since the higher frequency always leads to the smaller amplitude of oscillation, as described in the previous sections. This explains that a stable chaining formation is well preserved provided the field frequency is sufficiently low or high, e.g., $f = 1\,\mathrm{Hz}$ and $7\,\mathrm{Hz}$, whereas the structural instability occurs at the intermediate frequency $f = 3\,\mathrm{Hz}$ (see the formation pattern in Fig. 2). It is interesting to note that a transit mode of the chaining instability is found at $f = 5\,\mathrm{Hz}$ when the chain might be ruptured in the first few periods but remains stably chained afterwards (see the trajectory also shown in Fig. 3). To distinguish between this transition of the stably re-chained phenomenon and the continuously ruptured and re-chained behavior at $f = 3\,\mathrm{Hz}$, we name these two patterns as *re-chain* and *rupture*, respectively, in the following discussion.

We measured the oscillating amplitudes of the chains (θ_{Amax}) with different numbers of particles subjected to various field frequencies, as displayed in Fig. 4. The amplitude of the present oscillating field was theoretically calculated as $\theta_{\mathrm{fmax}} = 37.8°$. As reported in [34, 35, 37], a shorter chain, i.e. a smaller number N, always oscillates more prominently with a larger amplitude. This can be easily

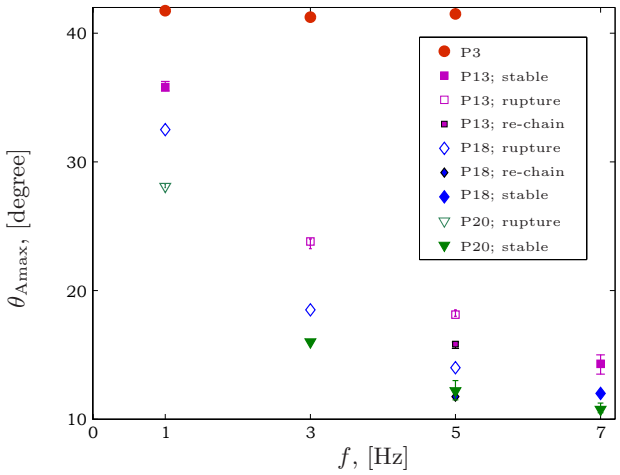

Fig. 4. Oscillation amplitudes (θ_{Amax}) for a chain consisting of different numbers of particles ($N = 3$, 13, 18 and 20) in various field frequencies. The field strength is fixed at $H_{\mathrm{d}} = 24.15\,\mathrm{Oe}$ and $H_{\mathrm{p}} = 18.73\,\mathrm{Oe}$. Except for the shortest P3 chain, the oscillation amplitude decreases monotonically with higher frequency.

understood by the induced viscous torque (M^{v}) approximated by [26]

$$M^{\mathrm{v}} = \frac{4\pi a^3 N}{3} \frac{2N^2}{\ln(N/2)} \eta\omega. \tag{3}$$

A longer chain always induces a stronger viscous drag to resist its oscillating motion. For the case of a very short P3 chain, the actual amplitude even exceeds the field because of the strong inertial effect [34]. Additionally, except this P3 chain, the smaller amplitude is always associated with the higher frequency, which is consistent with the previous observations. Note that the previously mentioned transition of the structural stability, i.e. the patterns of rupture, re-chain and stable chain, respectively, for a long, an intermediate and a short chain, is also confirmed. Because of their longer lengths, the P18 and P20 chains rupture at $f = 1\,\mathrm{Hz}$. By increasing further the frequency to reduce their amplitudes, the P18 and P20 chains resume to stable state at $f \geq 7\,\mathrm{Hz}$ and $f \geq 3\,\mathrm{Hz}$, respectively. In particular, the P18 chain appears at the transient mode of structural instability at $f = 5\,\mathrm{Hz}$ so that a re-chain pattern is observed.

To conclude this section, we perform a dimensional analysis. The results presented above clearly demonstrate that the oscillating amplitude depends strongly both on the length of the chain and on the frequency of the driving field. Moreover, the field strength also significantly affects the amplitude [34, 35, 37]. To generalize the influences of these factors, a dimensional analysis is desired. It is well understood that the motion of the chain is dominated by the magnetic driving force (M_{f}) and hydrodynamic drag (D_{f}). The magnetic force is represented as $M_{\mathrm{f}} \sim \mu_0 a^2 H^2$. The viscous drag for an N-particle chain, where N is large compared to unity, can be approximated by a modified Stokes drag as [25]

$$D_{\mathrm{f}} \sim \frac{2N^2}{log(N/2)} \eta a v,$$

where v is the velocity of particles. Since the angular velocity is proportional to the frequency, we assume $v \sim af$. The competition between the viscous drag (D_{f}) and the magnetic force (M_{f}), denoted as a dimensionless parameter f_{r}, can be expressed as

$$f_{\mathrm{r}} \sim \frac{D_{\mathrm{f}}}{M_{\mathrm{f}}} = \frac{2N^2}{\log(N/2)} \frac{\eta f}{\mu_0 H^2}. \tag{4}$$

It was observed that this new dimensionless parameter provides a similar physical interpretation of the conventional Mason number. Since the effect of the frequency is taken into account explicitly in this parameter, we name it as a *reduced frequency* for better presentation. To make the amplitude dimensionless, we normalize the amplitude of the oscillating chain by the corresponding field amplitude, so that the normalized amplitude can be expressed as

$$\theta_{\mathrm{n}} = \theta_{\mathrm{Amax}}/\theta_{\mathrm{fmax}}. \tag{5}$$

The dependence of these two dimensionless factors of the normalized amplitude (θ_{n}) on the reduced frequency (f_{r}) is illustrated in Fig. 5. It is emphasized that the data points in Fig. 5 include the results obtained under various experimental conditions reported in [34, 37], such that the conditions are extended to much more general situations, i.e. $9 \leq N \leq 21$, $14.6\,\mathrm{Oe} \leq H_{\mathrm{p}} \leq 163.3\,\mathrm{Oe}$, $1\,\mathrm{Hz} \leq f \leq 7\,\mathrm{Hz}$, and $\eta = 1.05\,\mathrm{cp}$ and $1.75\,\mathrm{cp}$. The normalized oscillating amplitude follows the generally decreasing trend with the increasing reduced frequency. The narrow spread of all the data points along a monotonic curve confirms the correctness of such dimensionless presentation.

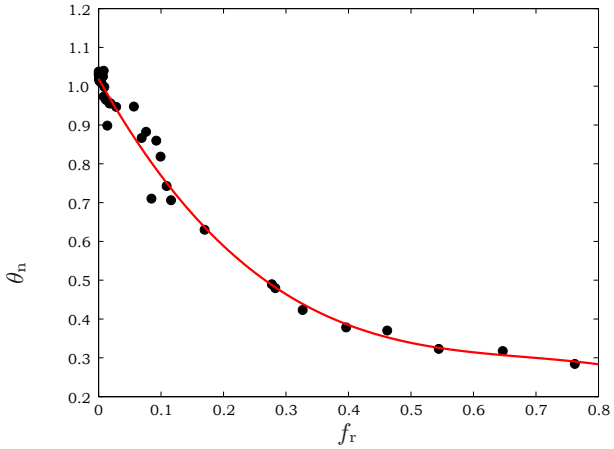

Fig. 5. The normalized amplitude of the oscillating chain (θ_n) vs. the dimensionless reduced frequency (f_r). The data points presented include results obtained under various experimental conditions reported in [34, 37], such as $N = 9-21$, $H_p = 14.6-163.3$ Oe, $f = 1-7$ Hz and $\eta = 1.05$ cp and 1.75 cp. The normalized oscillating amplitude follows a monotonically decreasing trend with increasing reduced frequency.

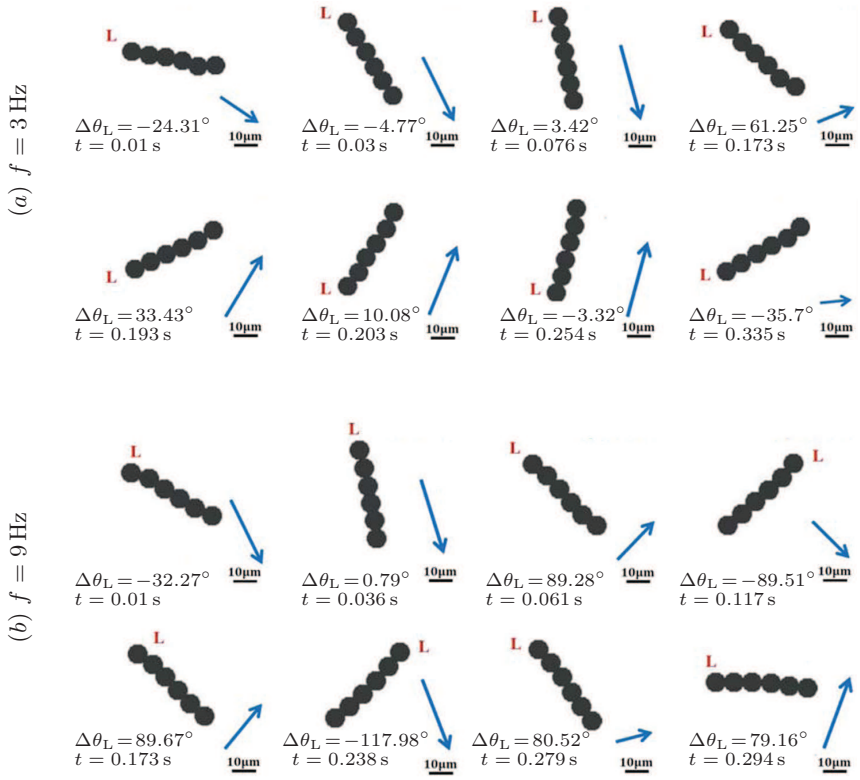

Fig. 6. Sequential images of a P6 chain subjected to the field frequency (*a*) $f = 3$ Hz (two top rows) and (*b*) $f = 9$ Hz (two bottom rows). Instantaneous strength and orientation of the external field are, respectively, represented by the length and direction of the arrow. For easier observation, the left-hand end of the initial chaining formation is marked by *L*. Since $|\Delta\theta_L| < 90°$ is always maintained for the case with the low frequency $f = 3$ Hz, the oscillating axis of the chain is consistent with the external field, i.e. along the horizontal axis of the directional field. On the other hand, the trajectory shift is triggered for the case $f = 9$ Hz shortly after $t = 0.061$ s, when the instantaneous $|\Delta\theta_L| > 90°$. The oscillating axis of the chain shifts to the vertical axis at $t = 0.061-0.279$ s.

2.2. Trajectory shift. Another issue concerned with the motion of the oscillating chain is the so-called trajectory shift [9, 35]. Instead of the oscillation along the directional field (horizontal $\mathbf{H}_\mathrm{d}$), e.g., cases shown in Fig. 2, the oscillating axis is shifted to follow along the vertical field $\mathbf{H}_\mathrm{p}$ when the magnetic torque changes its sign with $|\Delta\theta_\mathrm{L}| > 90°$, as expressed by Eq. (1). To trigger such a trajectory shift, an effective way is to increase the field amplitude (θ_fmax), since $\theta_\mathrm{fmax} = \tan^{-1}(H_\mathrm{p}/H_\mathrm{d})$. This is achieved by either increasing the vertical field strength H_p or weakening the directional field strength H_d [9, 35]. We demonstrate that the trajectory shift can also be triggered by raising the field frequency, even if the oscillating amplitude is decreased. Shown in Fig. 6 is the motion of a P6 chain subjected to the field strengths $H_\mathrm{d} = 38.15\,\mathrm{Oe}$ and $H_\mathrm{p} = 136.9\,\mathrm{Oe}$ with different frequencies $f = 3\,\mathrm{Hz}$ and $9\,\mathrm{Hz}$. For easier observation of the oscillating orientations, the left-hand end of the initial chaining formation is marked by L. Since $|\Delta\theta_\mathrm{L}| < 90°$ is always maintained for the case with the low frequency $f = 3\,\mathrm{Hz}$, the oscillating axis of the chain is consistent with the external field to follow the horizontal axis of the directional field, e.g., clockwise and counter-clockwise, respectively, within $t = 0-0.076\,\mathrm{s}$ and $t = 0.076-0.254\,\mathrm{s}$. On the other hand, the trajectory shift is triggered for the case with $f = 9\,\mathrm{Hz}$. Before $t = 0.061\,\mathrm{s}$, the chain follows the external field well to oscillate clockwise ($t = 0-0.036\,\mathrm{s}$) and counter-clockwise ($t = 0.036-0.061\,\mathrm{s}$). Nevertheless, a trajectory shift occurs shortly after $t = 0.061\,\mathrm{s}$ when the instantaneous $|\Delta\theta_\mathrm{L}|$ is close to 90°. At $t = 0.061-0.279\,\mathrm{s}$, the oscillating axis of the chain shifts toward the vertical axis, while the external field keeps oscillating along the horizontal axis. The trajectory shift triggered by the higher frequency can also be clearly identified by the phase trajectories shown in Fig. 7. Even if the trajectory phase of the chain exhibits a distinguishable lag to the field at $f = 3\,\mathrm{Hz}$, the two trajectories are consistent to oscillate along the horizontal axis, i.e. $\theta = 0°$. On the contrary, the trajectory of the chain with the

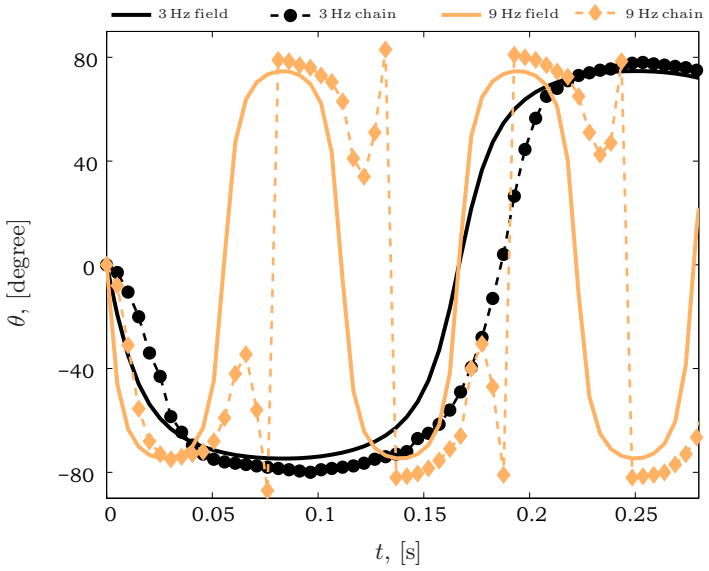

Fig. 7. Phase trajectories of the P6 chain and fields at $f = 3\,\mathrm{Hz}$ and $9\,\mathrm{Hz}$ shown in Fig. 6. For the case $f = 3\,\mathrm{Hz}$, its trajectory oscillates consistently with the field. On the contrary, the oscillating trajectory for the chain with the higher frequency $f = 9\,\mathrm{Hz}$ reverses immediately after $|\Delta\theta_\mathrm{L}|$ exceeding multiples of 90°.

higher frequency $f = 9\,\mathrm{Hz}$ oscillates oppositely to the external field shortly after $t = 0.061\,\mathrm{s}$. Afterwards, the chain oscillates along the vertical axis, i.e. $|\theta| = 90°$, while the external field keeps oscillating along the horizontal axis.

3. Concluding remarks. In the present study, influences of the field frequency driving an oscillating chain consisting of magnetic micro-particles are investigated. We first emphasize the effects of the field frequency on the dynamic patterns of the chain formation. Because of the resistance by the induced hydrodynamic drag, the motion of the chain always lags to the external field. The higher field frequency was found to lead sooner to the cross-over of the trajectories of the field and lagging chain. As a result, the amplitude of the oscillating chain reduces with higher field frequency. The reduced oscillating amplitude at the higher field frequency results in interesting transition of the chaining structural stability. On the one hand, the local angular velocity of the chain increases if the field frequency increases so that the chain is more likely to be ruptured apart during the oscillation. On the other hand, the smaller amplitude restricts the dramatic motion of the chain, and stable chaining formation is easier to preserve. Because of these two contradictory effects, the structural instability appears at an intermediate frequency. In addition, a newly identified transient mode, referred to as the re-chain phenomenon, was observed, in which the chain was ruptured in the first few periods of oscillation and remained stably chained afterward. As a result, a four-stage scenario regarding the structural stability, e.g., stable chain, ruptured chain, transient re-chain and stable chain, are possible by increasing the field frequency.

It is well understood that the main mechanisms acting upon the oscillating chain are the driving magnetic force and the hydrodynamic drag. To better elucidate all the parameters affecting these two forces, a dimensionless parameter, referred to as a reduced frequency, was proposed. The reduced frequency and the normalized amplitude of the oscillating chain demonstrated a monotonic dependence, in which the higher value of the reduced frequency generally leads to a smaller normalized amplitude. Finally, it was demonstrated that the trajectory shift, when the oscillating axis of the chain is aligned perpendicularly, can also be triggered by increasing the field frequency. In line with the reported findings in the literature, the trajectory is shifted at a time when the difference of trajectory phases between the chain and the field exceeds 90°.

4. Acknowledgments. Support by the Ministry of Science and Technology of the Republic of China (Taiwan) under grant MOST 104-2221-E-009-142-MY3 is acknowledged.

References

[1] N.T. Nguyen. Micro-magnetofluidics: interactions between magnetism and fluid flow on the microscale. *Microfluid Nanofluid*, vol. 12 (2012), p. 1.

[2] A. van Reenen, A.M. de Jong, J.M.J. den Toonder, M.W.J. Prins. Integrated lab-on-chip biosensing systems based on magnetic particle actuation V a comprehensive review. *Lab Chip*, vol. 14 (2014), p. 1966.

[3] B.Q. Cao, X. Han and L. Li. Configurations and control of magnetic fields for manipulating magnetic particles in microfluidic applications: magnet systems and manipulation mechanisms. *Lab Chip*, vol. 14 (2014), p. 2762.

[4] C. Goubault, P. Jop, M. Fermigier, J. Baudry, E. Bertrand and J. Bibette. Flexible magnetic filaments as micromechanical sensors. *Phys. Rev. Lett.*, vol. 91 (2003), p. 260802.

[5] A. Cebers. Flexible magnetic filaments. *Curr. Opin. Colloid Interface Sci.*, vol. 10 (2005), p. 167.

[6] R. Dreyfus, J. Baudry, M. Roper, M. Fermigier, H. Stone and J. Bibette. Microscopic artificial swimmers. *Nature*, vol. 437 (2005), p. 862.

[7] A. Cebers. Flexible magnetic swimmer. *Magnetohydrodynamics*, vol. 41 (2005), no. 1, pp. 63–72.

[8] Y.-H. Li, S.-T. Sheu, J.-M. Pai and C.-Y. Chen. Manipulations of oscillating micro magnetic particle chains. *J. Appl. Phys.*, vol. 111 (2012), p. 07A924.

[9] Y.-H. Li, H.-C. Lin and C.-Y. Chen. Steering of magnetic micro-swimmers. *IEEE Transactions on Magnetic*, vol. 49 (2013), no. 7, 4120.

[10] Y. Ido, Y.-H. Li, H. Tsutsumi, H. Sumiyoshi, and C.-Y. Chen. Magnetic microchains and microswimmers in an oscillating magnetic field. *Biomicrofluidics*, vol. 10 (2016), p. 011902.

[11] S. Biswal and A. Gast. Micromixing with linked chains of paramagnetic particles. *Anal. Chem.*, vol. 76 (2004), p. 6448.

[12] T.G. Kang, M. Hulsen, P. Anderson, J.M.J. den Toonder, H. Meijer. Chaotic mixing induced by a magnetic chain in a rotating magnetic field. *Phys. Rev.*, vol. E76 (2007), p. 066303.

[13] T. Roy T. A. Sinha, S. Chakraborty, R. Ganguly and I. Puri. Magnetic microsphere-based mixers for microdroplets. *Phys. Fluids*, vol. 21 (2009), p. 027101.

[14] I. Petousis, E. Homburg, R. Derks and A. Dietzel. Transient behaviour of magnetic micro-bead chains rotating in a fluid by external fields. *Lab Chip*, vol. 7 (2007), p. 1746.

[15] F. Lacharme, C. Vandevyver, M. Gijs. Magnetic beads retention device for sandwich immunoassay comparison of off-chip and on-chip antibody incubation. *Microfluid Nanofluid*, vol. 7 (2009), p. 479.

[16] A. Weddemann, F. Wittbracht, A. Auge, A. Hutten. Particle flow control by induced dipolar interaction of superparamagnetic microbeads. *Microfluid Nanofluid*, vol. 10 (2011), p. 459.

[17] M. Karle, J. Wohrle, J. Miwa, N. Paust, G. Roth, R. Zengerle, F. von Stetten. Controlled counter-flow motion of magnetic bead chains rolling along microchannels. *Microfluid Nanofluid*, vol. 10 (2011), p. 935.

[18] F. Wittbracht, A. Weddemann, B. Eickenberg, A. Hutten. On the direct employment of dipolar particle interaction in microfluidic system. *Microfluid Nanofluid*, vol. 13 (2012), p. 543.

[19] S. Melle, G. Fuller, M. Rubio. Structure and dynamics of magnetorheological fluids in rotating magnetic fields. Phys. Rev., vol. E61 (2000), p. 4111.

[20] S. Melle, O. Calderon, G. Fuller, M. Rubio. Polarizable particle aggregation under rotating magnetic fields using scattering dichroism. *J. Colloid Interface Sci.*, vol. 247 (2002), p. 200.

[21] S. Melle, O. Calderon, M. Rubio, G. Fuller. Rotational dynamics in dipolar colloidal suspensions: video microscopy experiments and simulations results. *J. Non-Newton Fluid Mech.*, vol. 102 (2002), p. 135.

[22] S. Melle, O.G. Calderon, M.A. Rubio and G.G. Fuller. Microstructure evolution in magnetorheological suspensions governed by Mason number. *Phys. Rev.*, vol. E68 (2003), p. 041503).

[23] S. Melle and J.E. Martin. Chain model of a magnetorheological suspension in a rotating field. *J. Chem Phys.*, vol. 118 (2003), p. 21.

[24] A. Vuppu, A. Garcia, M. Hayes. Video microscopy of dynamically aggregated paramagnetic particle chains in an applied rotating magnetic field. *Langmuir*, vol. 19 (2003), p. 8646.

[25] C. Wilhelm, J. Browaeys, A. Ponton, J.-C. Bacri. Rotational magnetic particles microrheology: The Maxwellian case. *Phys. Rev.*, vol. E67 (2003), p. 011504.

[26] S. Biswal and A. Gast. Rotational dynamics of semiflexible paramagnetic particle chains. *Phys. Rev.*, vol. E69 (2004), p. 041406.

[27] A. Cebers and I. Javaitis. Dynamics of a flexible magnetic chain in a rotating magnetic field. *Phys. Rev.*, vol. E69 (2004), p. 021404.

[28] A. Cebers, M. Ozols. Dynamics of an active magnetic particle in a rotating magnetic field. *Phys. Rev.*, vol. E73 (2006), p. 021505.

[29] K. Erglis, D. Zhulenkovs, A. Sharipo, A. Cebers. Elastic properties of DNA linked flexible magnetic filaments. *J. Phys.: Condens. Matter*, vol. 20 (2008), p. 204107.

[30] B. Frka-Petesic, K. Erglis, J.F. Berret, A. Cebers, V. Dupuis, J. Fresnais, O. Sandre, R. Perzynski. Dynamics of paramagnetic nanostructured rods under rotating field. *J. Magnetism and Magn. Mat.*, vol. 323 (2011), p. 1309.

[31] U. Banerjee, P. Bit, R. Ganguly, S. Hardt. Aggregation dynamics of particles in a microchannel due to an applied magnetic field. *Microfluid Nanofluid*, vol. 13 (2012), p. 565.

[32] Y. Gao, M.A. Hulsen, T.G. Kang and J.M.J. Den Toonder. Numerical and experimental study of a rotating magnetic particle chain in a viscous fluid. *Phys. Rev.*, vol. E86 (2012), p. 041503.

[33] L.D. Yepez, J.L. Carrillo, F. Donado, J.M. Sausedo-Solorio, P. Miranda-Romagnoli. Dynamical pattern formation in a low-concentration magnetorheological fluid under two orthogonal sinusoidal fields. *J. Magnetism and Magn. Mat.*, vol. 408 (2016), p. 321.

[34] Y.-H. Li, C.-Y. Chen, S.-T. Sheu and J.-M. Pai. Dynamics of a microchain of superparamagnetic beads in an oscillating field. *Microfluid Nanofluid*, vol. 13 (2012), p. 579.

[35] Y.-H. Li, H.-C. Lin and C.-Y. Chen. Trajectory shift of magnetic microchains in an oscillating field. *Microfluid Nanofluid*, vol. 14 (2013), p. 831.

[36] Y.-H. Li, E. Bansal and C.-Y. Chen. Breakups of magnetic chains in an oscillating field. *Magnetohydrodynamics*, vol. 50 (2014), no. 1, pp. 19–26.

[37] H.-C. Lin, Y.-H. Li and C.-Y. Chen. Structural instability of an oscillating superparamagnetic micro-bead chain. *Microfluid Nanofluid*, vol. 17 (2014), p. 73.

Received 24.05.2017